JOURNAL OF SOLID STATE CHEMISTRY 113, 225–228 (1994)

Hysteretic Evidence for Finite Ordered Domains in Continuous Verwey Transformations

Ricardo Aragón[1]

Department of Chemical Engineering, University of Delaware, Newark, Delaware 19716

and

John W. Koenitzer

Department of Chemistry, Northwestern University, Evanston, Illinois 60208

Received July 28, 1993; accepted October 22, 1993

Low temperature x-ray diffraction experiments on $Fe_{3(1-\delta)}O_4$ single crystals ($\delta = 0.0045$) with a modified precession camera reveal diffraction patterns indexable with the same base centered monoclinic unit cell of stoichiometric Fe_3O_4. The intensity at (8 0 $\frac{1}{2}$), representative of the characteristic doubling of the spinel unit cell associated with Verwey ordering, increases gradually below a transformation temperature ($T_V^{II} = 99$ K) consistently with the continuous character observed for $\delta > \delta_C = 0.0039$, in marked contrast with the discontinuous appearance of half-integer Bragg reflections below the first-order transition ($T_V^{I} = 122$ K) for $\delta = 0$. Thermal hysteresis is observed in the satellite intensity beyond the percolation limit (δ_C), which correlates with similar behavior in electrical resistivity and provides evidence for the existence of finite ordered domains.

INTRODUCTION

The charge ordering transition observed in magnetite ($Fe_{3(1-\delta)}O_4$) below $T_V = 122$ K has received sustained attention since its original description by Verwey and Haajman (1) in 1941. Although the specific structural model originally proposed for the low temperature phase has since been disproved, there is no doubt that it results from ordering of the Fe^{2+} and Fe^{3+} cations in the octahedral (B) sublattice of the parent cubic inverse spinel structure. Electron and neutron diffraction studies showed that the appearance of superlattice peaks below T_V, at (h, 0, $l + \frac{1}{2}$), results from atomic displacements, attributed to the coupling of charge ordering and lattice phonons (2).

Systematic investigations of the influence of metal–oxygen nonstoichiometry (δ) on Verwey ordering confirmed that T_V is markedly depressed with increasing δ, and specific heat measurements (3) showed that the latent heat of the transition is suddenly lost, for cation deficiency in excess of a critical composition $\delta_C = 0.0039$, in an apparent (4) discontinuous change from first (T_V^{I}) to second (T_V^{II}) order. The observation of thermal hysteresis effects associated with continuous transformations beyond this critical composition, which are absent in the discontinuous regime, seems inconsistent with a second-order transition and motivates this investigation of related structural changes.

EXPERIMENTAL

$Fe_{3(1-\delta)}O_4$ single crystals, grown by skull melting (5) from 99.999% pure Fe_2O_3 reagent, were annealed under controlled oxygen fugacity conditions by techniques described elsewhere (6) to produce δ values of 0.000 and 0.0045, respectively corresponding to a stoichiometric composition, with a first order Verwey transition ($T_V^{I} = 122$ K), and cation deficiency beyond δ_C, for which a continuous transformation ($T_V^{II} = 99$ K) is observed. The crystals were oriented by Laue back reflection techniques to cut slabs parallel to (1 0 0), which were ground to a thickness of 140 μm by standard lapidary methods, determined to be the optimum $2/\mu$, for a linear absorption coefficient $\mu = 146$ (cm^{-1}), computed (7) for MoK_α radiation.

An Elliot 15 kW (nominal) rotating anode, fitted (8) with a pivoting table and a displaceable flat graphite monochromator on its exit port, was used to generate the white and monochromatic MoK_α beams for orientation and precession photographs, respectively, with a Huber model 205 camera. Typical conditions were 200 mA at 30 kV to avoid excitation of $\lambda/2$ radiation. Multiple exposures of limited scans on a single plate were made possible by calibrated displacements of the film cassette.

A controlled low temperature ($78 > T > 300$ K) sample support was provided with a miniature Joule–Thomson

[1] To whom correspondence should be addressed.

0022-4596/94 $6.00

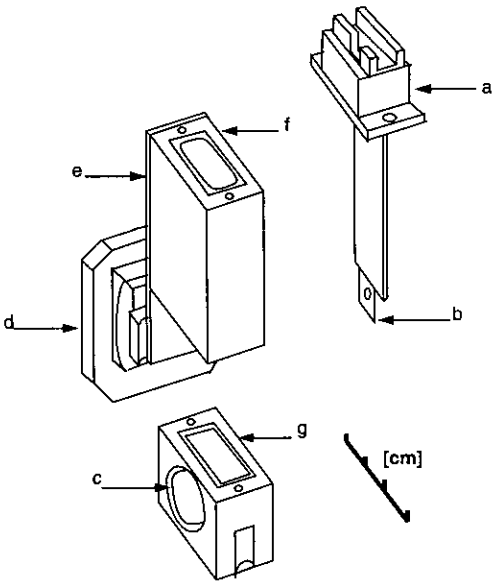

FIG. 1. Isometric expanded view of the cryogenic sample mount: MMR model 770 Joule–Thomson refrigerator (a); oxygen-free copper stage for sample and Si diode support (b); beryllium window (c); Huber 1006 goniometer head (d); stainless steel support and main vacuum chamber (e); gasket seals (f, g).

refrigerator (MMR Technologies 770) equipped with a calibrated Si diode sensor, mounted on an oxygen-free copper sample stage. A two-piece aluminum vacuum chamber (cf. Fig. 1) was designed with gasketed surfaces, which allow the removal of a lower cap, fitted with dual 0.1-mm-thick beryllium windows for optical alignment of the crystal. The chamber was secured to a goniometer head (Huber 1006a), compatible with the standard camera mounting, and evacuated to 10^{-6} Torr with an oil diffusion pump.

Continued operation of the refrigerator, for exposures in excess of 20 hr, required a high pressure (1800 psi) liquid nitrogen foreline trap for removal of CO_2 and moisture contamination from the nitrogen feed gas. Thermal stability, using a Lake Shore DRC500 controller, was better than 0.05 K and the accuracy of the thermometry was better than 0.1 K, with a resolution of 0.01 K.

The well-established (9) field cooling technique was employed to set the c axis of the low temperature phase on a cubic [1 0 0] direction, predetermined by the Laue orientation to correspond to the horizontal goniometric axis. Rare-earth–cobalt permanent magnet disks or rings, attached to the lower cap of the vacuum chamber, provided the required magnetic field, parallel or normal to the crystal oscillation axis, respectively. No attempt was made to inhibit basal twinning.

RESULTS AND DISCUSSION

A zero layer photograph, representative of a set including $\zeta = 0, \frac{1}{2}, 1$, and 2, for $\delta = 0.0045$ at 78 K, is shown in Fig. 2. All observed Bragg reflections are indexable with the same base-centered monoclinic unit cell ($\sqrt{\mathbf{a}}$, $\sqrt{\mathbf{a}}$, $2\mathbf{a}$), observed for stoichiometric magnetite, characterized by the appearance of $(h\ 0\ l + \frac{1}{2})$ satellites along the magnetic field determined cubic [0 0 1] axis.

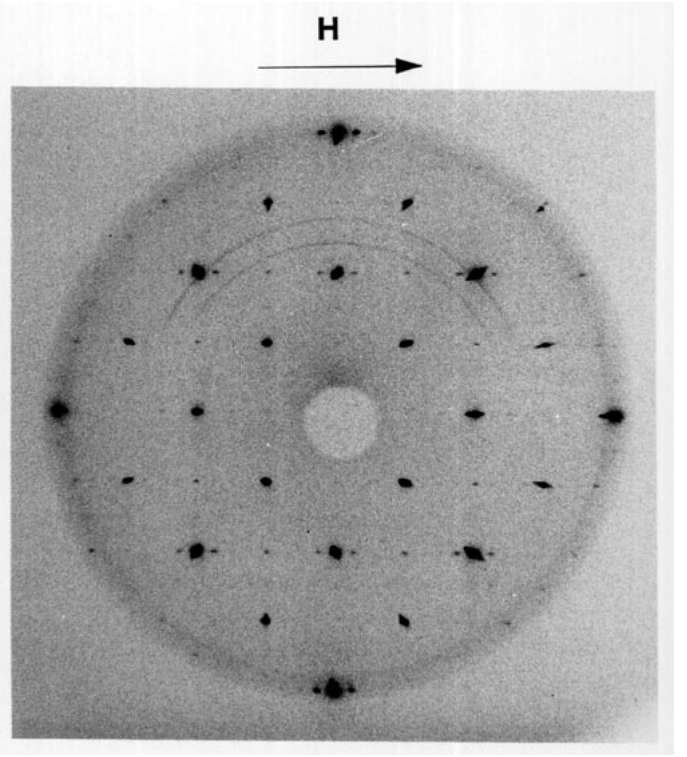

FIG. 2. Zero order precession photograph. $\delta = 0.0045$, $T = 78$ K, transverse magnetic field (H), MoK_α, 30 kV, 180 mA, 407 precessions, $\mu = 20°$ (rings due to contamination from diffraction by the sample holder).

The difference between the samples above and below δ_C is manifest in the temperature dependence of the half-integer satellite intensity. The (8 0 0) reflection and its two satellites, (8 0 $\frac{1}{2}$) and (8 0 $\bar{\frac{1}{2}}$), were selected for monitoring, setting the precession angle to $\mu = 20°$ and the oscillation switches to $\pm 5°$. Calibrated displacements of the film cassette after each exposure were used to record multiple scans on a single plate.

For $\delta = 0.0045$, a gradual and continuous increase in the satellite intensity was evident below $T_V^{II} = 99$ K (cf. Fig. 3) consistently with continuous character. The photographs were digitized with a scanning microdensitometer and the integrated satellite intensities were evaluated on a single relative scale, using common control reflections in each plate. Thermal hysteresis of ~2 K was observed in the range 93 K $< T < T_V^{II}$ (cf. Fig. 4), in close correlation with similar effects in dc electrical resistivity (cf. Fig. 5) and prior calorimetric investigations.

The observation of $(h\ 0\ l + \frac{1}{2})$ satellites for $\delta > \delta_C$ indicates a common diffraction pattern for the low tem-

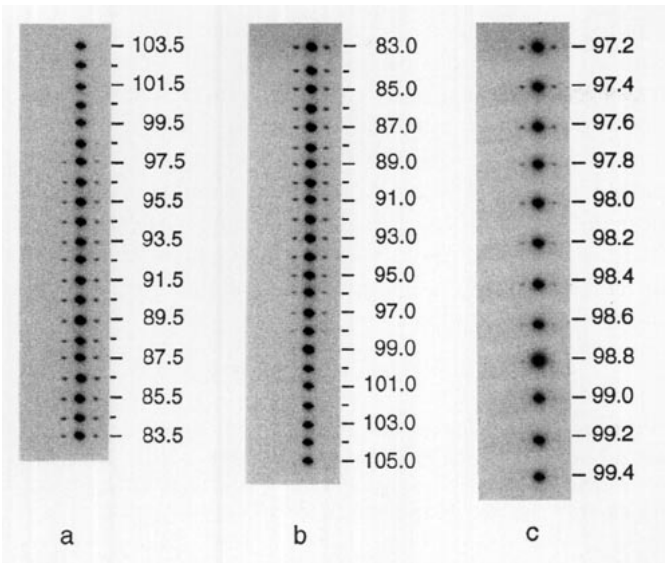

FIG. 3. (8 0 ½) satellites for $\delta = 0.0045$, as a function of temperature for cooling ((a): 407 oscillations, (b): 780 oscillations) and heating ((c): 407 oscillations) cycles. Other conditions as in Fig. 2; precession stops at ±5°.

perature phase, irrespective of the order of the Verwey transformation, thus excluding the possibility of a simple cell preserving (10) transition for the continuous regime. The requisite absence of cubic invariants in the potential expansion for a second-order transition restricts (11) the reduction of symmetry operators in the low temperature phase to a subgroup of the parent form by the well-established (12) subduction condition. The only alternative to this constraint requires the presence of symmetry breaking terms.

Recent neutron scattering experiments (13) have demonstrated the breaking of translational symmetry for $\delta > \delta_C$, with evidence that the half-integer superlattice peaks observed upon cooling below T_V^{II} never become resolution limited and consequently, that long range order (LRO) is not attained at any temperature. In the absence of an infinite correlation length, there is no true phase transition.

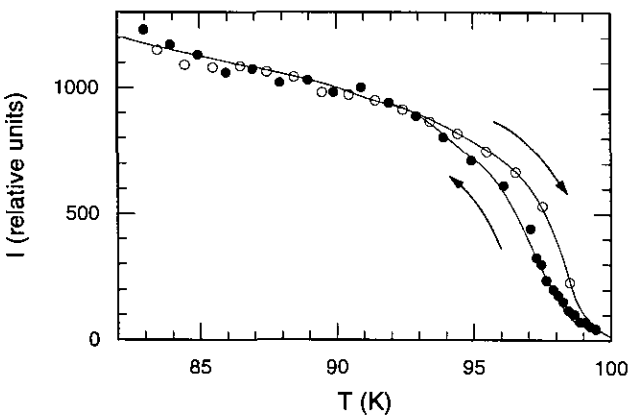

FIG. 4. Average of the densitometric integrated intensity (cf. Fig. 3) for the two (8 0 ½) satellites as a function of temperature.

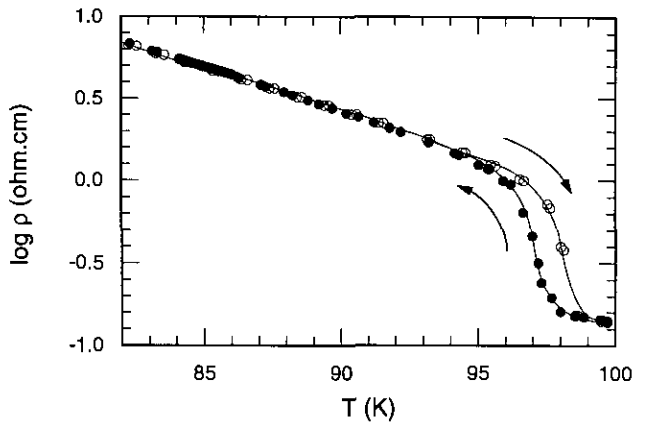

FIG. 5. Four probe dc electrical resistivity measurements on a single crystal cycled twice across its continuous Verwey transformation ($T_V^{II} = 99$ K).

The absence of LRO is consistent with a composition in excess of the percolation limit, beyond which the transition is inhibited by insufficient average charge per ordered unit cell. Simple stoichiometric considerations demonstrate that for $\delta > \delta_C$, the induced charge deficiency cannot sustain long-range charge ordering below T_V^{II}. The pertinent point defect equilibrium reactions in $Fe_{3(1-\delta)}O_4$ are (14)

$$Fe \rightarrow V + I \qquad [1]$$

for the formation of a vacancy Frenkel vacancy (V) interstitial (I) pair and

$$Fe^{2+} + \tfrac{1}{4} \cdot O_2 \rightarrow Fe^{3+} + \tfrac{1}{2} \cdot O^{2-} + \tfrac{3}{8} \cdot V \qquad [2]$$

$$Fe^{2+} + \tfrac{1}{4} \cdot O_2 + \tfrac{3}{8} \cdot I \rightarrow Fe^{3+} + \tfrac{1}{2} \cdot O^{2-} \qquad [3]$$

for the equivalent formation of vacancies or assimilation of interstitials by oxidation of one Fe^{2+} to Fe^{3+}. The stoichiometric fraction (δ) is determined by mass balance, with the difference of the number of vacancies and interstitials divided by the appropriate normalizing summation of cation and vacant sites (n_Σ):

$$\delta = \frac{1}{n_\Sigma} \cdot (n_V - n_I), \qquad [4]$$

thus excluding equilibrium defects associated only with thermal Frenkel disorder, and inspection of Eqs. [2] and [3] shows that electroneutrality is preserved if:

$$n_V - n_I = \tfrac{1}{8} \cdot (n_{Fe^{3+}} - 2 \cdot n_{Fe^{2+}}). \qquad [5]$$

Consequently, the average loss of one electron, associated with the oxidation of one Fe^{2+} to Fe^{3+}, of the $n_\Sigma = 96$ cations in the low temperature base-centered monoclinic unit cell (i.e., $\sqrt{\mathbf{a}}$, $\sqrt{\mathbf{a}}$, $2\mathbf{a}$, where $\mathbf{a}$ is the spinel cubic unit cell parameter) corresponds to $\delta_C = 0.0039$ by substitution into Eqs. [4] and [5]. Beyond this critical stoichiometry, the ordered domain size is finite and decreases proportionally to increasing δ. The transformation at T_V^{II} occurs when the thermally dependent correlation length equals the compositionally dependent maximum ordered domain size (13). Further decrease of temperature increases the number of ordered clusters and hence the intensity of the half-integer diffraction satellites but does not change their size, which is determined by δ, leading to broad, temperature-independent peak widths.

A clear distinction exists between the thermal hysteretic phenomena below T_V^{II} and those associated with discontinuous transitions. Fundamentally, hysteresis ensues whenever the reversal of the process control variables (e.g., temperature) does not retrace the path of the essential variable (e.g., the order parameter) in state space. For first-order transitions associated with a simple cusp catastrophe (15), the delay limits are determined by the divergence away from the cusp or "pucker" point of the semicubical parabolic bifurcation set, which is symmetric about its major axis (i.e., the Maxwell set of discontinuous transitions). No hysteresis is predicted for the isolated second-order transition at the cusp, where the divergence is zero.

Whether hysteresis actually occurs or not in a first-order transition depends on the mechanism of the transformation (16). In fact, such effects are not significant for discontinuous Verwey transitions, since the observed hysteresis is smaller (17) than the width of the transition. Whenever hysteresis exists, the topological constraints require that the heating and cooling observations bracket the Maxwell transition at their midpoint. This is clearly not the case in the continuous regime ($\delta > \delta_C$), where the transformation temperature (T_V^{II}), assigned to the discontinuous change in the first derivative of the empirical order parameter pertinent to the monitored property, is coincident for heating and cooling; the hysteretic path difference is observed below this temperature (cf. Figs. 4 and 5). Similarly, the topological constraints (16) for the existence of hysteresis after a single bifurcation do not apply to T_V^{II} because correlation length and cluster size are associated with two independent divergences.

Regardless of their physical origin, the existence of discommensurations in ferroelectric materials, such as (I8) $NaNO_2$ and (I9) K_2SeO_4, or charge density wave compounds, such as 20 TaS_3, induces thermal hysteretic effects below the associated ordering transformations, similar to those described here for T_V^{II}. The common feature in all these cases is a statistical distribution of ordered domains, modeled (21) as the "devil's staircase" in commensurate–incommensurate structures, where the pattern of growth is not governed by a single-valued function of temperature. Evidence of thermal hysteresis in these instances, associated with nonresolution limited diffraction peaks, is diagnostic for the presence of a finite ordered intergrowth.

ACKNOWLEDGMENTS

The authors are indebted to Professor R. Colella for his expert advice and access to a rotating anode X-ray port, to Professor H. O. A. Meyer for the use of a precession goniometer, and to Professor M. Rossmann for the scanning microdensitometry. This work was initially supported by the National Science Foundation under Grant DMR-86-16533.

REFERENCES

1. E. J. Verwey and P. W. Haajman, *Physica (Utrecht)* **8,** 979 (1941); E. J. Verwey, P. W. Haayman, and F. C. Romejin, *J. Chem. Phys.* **15,** 181 (1947).
2. T. Yamada, K. Suzuki, and S. Chikazumi, *Appl. Phys. Lett.* **13,** 172 (1968); E. J. Samuelsen, E. J. Bleeker, L. Dobrzynski, and T. Riste, *J. Appl. Phys.* **39,** 114 (1968).
3. J. P. Shepherd, R. Aragón, J. W. Koenitzer, and J. M. Honig, *Phys. Rev. B* **32,** 1818 (1985).
4. R. Aragón and J. M. Honig, *Phys. Rev. B* **37,** 209 (1988); J. P. Shepherd, J. W. Koenitzer, R Aragón, J. Spatek, and J. M. Honig *Phys. Rev. B* **43,** 8461 (1991).
5. H. R. Harrison and R. Aragón, *Mater. Res. Bull.* **13,** 1097 (1978).
6. R. Aragón, D. J. Buttrey, J. P. Shepherd, and J. M. Honig, *Phys. Rev. B* **31,** 430 (1985).
7. "International Tables for X-Ray Crystallography," Vol. 3, p. 161. Reidel, Dordrecht, 1985.
8. L. D. Chapman and R. Colella, *Phys. Rev. B* **32,** 2233 (1985).
9. C. A. Domenicali, *Phys. Rev. B* **78,** 458 (1950).
10. J. L. Birman, *Phys. Rev. Lett.* **17,** 1216 (1966).
11. L. D. Landau and E. M. Lifschitz, "Statistical Physics," p. 439. Pergamon, Oxford, 1959.
12. J. Kocinski, "Theory of Symmetry Changes at Continuous Phase Transitions," p. 1987. Elsevier, Amsterdam, 1983.
13. R. Aragón, P. M. Gehring, and S. M. Shapiro, *Phys. Rev. Lett.* **70,** 1635 (1993).
14. H. Flood and D. G. Hill, *Z. Elektrochem.* **61,** 18 (1957); R. Aragón, D. J. Buttrey, J. P. Shepherd, and J. M. Honig, *Phys. Rev. B* **31,** 430 (1985).
15. T. Poston and I. Stewart, "Catastrophe Theory and its Applications," p. 85. Pitman, London, 1978.
16. C. Tesser and P. Coullet, *J. Phys. Lett.* **41,** L243 (1980).
17. J. P. Shepherd, J. W. Koenitzer, R. Aragón, C. J. Sandberg, and J. M. Honig, *Phys. Rev. B* **31,** 1107 (1985).
18. H. Böhm, *Am. Mineral.* **68,** 11 (1983).
19. M. Izumi, J. D. Axe, G. Shirane, and K. Shimaoka, *Phys. Rev. B* **15,** 4392 (1977).
20. A. W. Higgs and J. C. Gill, *Solid State Commun.* **47,** 737 (1983).
21. P. Bak, *Rep. Prog. Phys.* **45,** 587 (1982).